



## OPEN Characteristics of autosomal dominant *WFS1*-associated optic neuropathy and its comparability to *OPA1*-associated autosomal dominant optic atrophy

Cansu de Muijnck<sup>1,2</sup>, Lonneke Haer-Wigman<sup>3</sup>, Judith A. M. van Everdingen<sup>4</sup>, Tanya Lushchik<sup>4</sup>, Pam A. T. Heutinck<sup>5</sup>, Marieke F. van Dooren<sup>6</sup>, Anneke J. A. Kievit<sup>6</sup>, Virginie J. M. Verhoeven<sup>5,6</sup>, Marleen E. H. Simon<sup>7</sup>, Rosemarie A. Wasmann<sup>8</sup>, Irene C. Notting<sup>9</sup>, Elfride De Baere<sup>10,11</sup>, Sophie Walraedt<sup>12</sup>, Julie De Zaeytijd<sup>12</sup>, Filip Van den Broeck<sup>12,13</sup>, Bart P. Leroy<sup>10,12,13</sup>, Camiel J. F. Boon<sup>2,9</sup> & Maria M. van Genderen<sup>1,14</sup>✉

This study aims to describe the ophthalmic characteristics of autosomal dominant (AD) *WFS1*-associated optic atrophy (AD *WFS1*-OA), and to explore phenotypic differences with dominant optic atrophy (DOA) caused by mutations in the *OPA1*-gene. *WFS1*-associated diseases, or 'wolframopathies', exhibit a spectrum of ocular and systemic phenotypes, of which the autosomal recessive Wolfram syndrome has been the most extensively studied. AD mutations in *WFS1* also cause various phenotypical changes including OA. The most common phenotype in AD *WFS1*-associated disease, the combination of OA and hearing loss (HL), clinically resembles the 'plus' phenotype of DOA. We performed a comprehensive medical record review across tertiary referral centers in the Netherlands and Belgium resulting in 22 patients with heterozygous *WFS1* variants. Eighteen (82%) had HL in addition to OA. Diabetes mellitus was found in 7 (32%). Four patients had isolated OA. One patient had an unusual phenotype with anterior chamber abnormalities and malformations of the extremities. Compared to DOA, AD *WFS1*-OA patients had different color vision abnormalities (red-green vs blue-yellow in DOA), abnormal OPL lamination on macular OCT (absent in DOA), more generalized thinning of the retinal nerve fiber layer, and more reduced and delayed pattern reversal visual evoked potentials.

**Keywords** *WFS1*, Optic atrophy, *OPA1*, DOA, Inherited optic neuropathy

*WFS1*(NM-006005.3) was first described in 1998 as the disease-associated gene for the autosomal recessive (AR) severe multisystem disease Wolfram syndrome, which is characterized by optic atrophy (OA), diabetes mellitus

<sup>1</sup>Department of Ophthalmology, University Medical Center Utrecht, Utrecht, The Netherlands. <sup>2</sup>Department of Ophthalmology, Amsterdam University Medical Centers, Amsterdam, The Netherlands. <sup>3</sup>Department of Human Genetics, Radboud University Medical Center, Nijmegen, The Netherlands. <sup>4</sup>Department of Neuro-Ophthalmology, The Rotterdam Eye Hospital, Rotterdam, The Netherlands. <sup>5</sup>Department of Ophthalmology, Erasmus MC University Medical Center, Rotterdam, The Netherlands. <sup>6</sup>Department of Clinical Genetics, Erasmus MC University Medical Center, Rotterdam, The Netherlands. <sup>7</sup>Department of Genetics, University Medical Center Utrecht, Utrecht, The Netherlands. <sup>8</sup>Department of Ophthalmology, University Medical Center Groningen, University of Groningen, Groningen, The Netherlands. <sup>9</sup>Department of Ophthalmology, Leiden University Medical Center, Leiden, The Netherlands. <sup>10</sup>Center for Medical Genetics, Ghent University Hospital, Ghent University, Ghent, Belgium. <sup>11</sup>Department of Biomolecular Medicine, Ghent University, Ghent, Belgium. <sup>12</sup>Department of Ophthalmology, Ghent University Hospital, Ghent, Belgium. <sup>13</sup>Department of Head and Skin, Ghent University, Ghent, Belgium. <sup>14</sup>Bartiméus Diagnostic Center for Complex Visual Disorders, Zeist, The Netherlands. ✉email: mvgenderen@bartimeus.nl

(DM), diabetes insipidus, and sensorineural hearing loss (HL)<sup>1,2</sup>. In the last decade, new data showed that not only biallelic variants but also monoallelic variants in *WFS1* are associated with disease manifestations<sup>3</sup>. *WFS1*-associated diseases or as we previously proposed to name, *wolframopathies*, encompass a disease spectrum, ranging from relatively mild autosomal dominant (AD) Wolfram-like syndrome (WFLS), to the more severe presentation of autosomal recessive Wolfram syndrome (AR-WS)<sup>4</sup>.

The ophthalmic phenotype of AR-WS has been relatively well-described throughout the years<sup>5,6</sup>. However, because the association between AD *WFS1* variants and optic atrophy has only recently been discovered, the number of studies describing ophthalmic characteristics of AD *WFS1*-associated optic neuropathy (AD *WFS1*-OA) is still limited<sup>3,7,8</sup>. Yet, recent data show that heterozygous *WFS1* variants are the second most commonly detected variants in AD inherited optic neuropathy (inherited ON)<sup>9</sup>. More studies on AD *WFS1*-OA are needed for delineation of clinical symptoms, clinical variability, and long-term visual outcome, to aid in early diagnosis and prognostication.

In a recent systematic review on WFLS, we described the combination of OA and HL as a common phenotype in AD *WFS1* variants. While patients with AD *WFS1* variants have a risk of developing other clinical manifestations such as DM, the majority of the patients in this systematic review had only OA and HL<sup>4</sup>. These findings show similarities to autosomal dominant optic atrophy (DOA) associated with *OPA1* variants, especially to the DOA “plus” phenotype, and can be difficult to differentiate in clinical practice. In the current study, we describe the ophthalmic characteristics of 21 patients with AD *WFS1*-OA (plus 1 patient with unconfirmed OA but an unusual ocular phenotype) and provide a comparison of these findings to DOA through an age matched DOA cohort with genetically confirmed *OPA1* variants.

## Results

### Patients

We included in total 22 patients. Median follow-up time was 5 years (range 0–26). A summary of the demographics of the included patients is presented in Table 1.

### Genetic characteristics

In total, 13 disease-associated single heterozygous variants in the *WFS1* gene were detected. The p.Ala684Val variant was most common (n = 10, 45%). Except for one (p.(Gln668\*)), all the variants in this cohort were missense variants. A summary of the variants with the associated phenotypic features is presented in Table 2. Details of the pathogenicity assessment of the variants are reported in supplementary Table 1.

Eighteen patients in the study cohort had HL (82%). Of these 18 patients, 8 had a cochlear implant (CI), 1 patient non-CI hearing aids, and 6 patients no hearing aid in any form. Five of these 6 patients were the oldest in the cohort and profoundly deaf. The youngest patient was a baby and was not yet fitted with a CI. Information on CI status of 3 patients was absent the patient files. Seven patients (32%) were diagnosed with DM. None of the patients exhibited diabetes insipidus. Other non-ophthalmologic features included growth retardation (3; 14%), precocious puberty and developmental delay (1; 5%), low intellect and microcephaly (1; 5%), premature ovarian failure (1; 5%), primary hyperparathyroidism (1; 5%), ataxia and depression (1; 5%), tremor (1; 5%), paresthesia (1; 5%); bilateral clubfoot, thumb contracture, windblown fingers, and persisting left superior vena cava (combined in 1 patient; 5%).

Patient 20 had congenital HL, OA (9), and DM (5), and genetic analysis in 2001 revealed compound heterozygosity for two *WFS1* variants. On her last follow-up, we saw outer plexiform layer (OPL) lamination on macular OCT, a finding thus far only described for AD *WFS1*-associated disease. Considering the changes in the variant classification guidelines over the years, and the additional information available for variant classification, we requested a re-evaluation of the variants which resulted in one variant classified as likely benign (c.683G > A p.(Arg228His)), and one as likely pathogenic (c.2430C > A p.(Phe810Leu)). Together with the segregation

Demographics	Subjects, n = 22
Age, mean [range]	35.7 [0–78]
Sex, n (%)	
Female	14 (63.6%)
Male	8 (36.4%)
Country of origin	
The Netherlands	13 (59.1%)
Belgium	3 (13.6%)
Afghanistan	1 (4.5%)
Guinea Conakry	1 (4.5%)
Bangladesh	1 (4.5%)
Bolivia	1 (4.5%)
Germany	1 (4.5%)
Morocco	1 (4.5%)

**Table 1.** Demographics of the included patients.

Patient	Variant	Variant class	Age	Gender	Phenotype (age at onset in years)	Notes
1	c.937C>T p.(His313Tyr)	5	6	M	OA (5), DM (1), HL (0)	
2	c.[991_993del;1597C>T] p.[(Phe331del);(Pro533Ser)], de novo (cis)	4	32	F	OA (32), HL (0), cataract (3)	Pathogenicity assessed for the allele, not individually for the variants
3	c.1672C>T p.(Arg558Cys)	5	70	F	OA (25)	
4	c.2002C>T p.(Gln668*)	5	66	F	OA (52), essential tremor (unknown)	
5	c.2044A>G p.(Asn682Asp)	3	70	M	OA (67), DM (66), HL (0)	
6	c.2051C>T p.(Ala684Val)	5	54	F	OA (24), HL (0)	
7	c.2051C>T p.(Ala684Val)	5	19	F	OA (4), HL (0)	
8	c.2051C>T p.(Ala684Val)	5	8	M	OA (4), HL (0)	
9	c.2051C>T p.(Ala684Val)	5	77	M	OA (25), DM (15), HL (0), cataract (32), ataxia (52), depression (unknown)	
10	c.2051C>T p.(Ala684Val)	5	29	F	OA (10), HL (0)	
11	c.2051C>T p.(Ala684Val)	5	21	M	OA (13), DM (13), HL (0), borderline mental retardation, low height, microcephaly	
12	c.2051C>T p.(Ala684Val)	5	23	F	OA (5), DM (12), HL (0), premature ovarian failure (12), growth retardation (5)	
13	c.2051C>T p.(Ala684Val)	5	5	F	OA (5), HL (2)	
14	c.2051C>T p.(Ala684Val)	5	16	F	OA (5), HL (3), growth hormone deficiency (unknown)	
15	c.2051C>T p.(Ala684Val)	5	51	F	OA (22), HL (4), paraesthesia (52)	
16	c.2213C>A p.(Ala738Asp)	4	59	F	OA (39)	
17	c.2389G>A p.(Asp797Asn)	4	78	M	OA (63), HL (0)	
18	c.2389G>T p.(Asp797Tyr)	4	40	M	OA (12), HL (0)	
19	c.2425G>A p.(Glu809Lys)	5	0	M	Anterior segment abnormalities, DM (0), HL (0) bilateral club feet, thumb contracture, windblown fingers, and persisting left superior vena cava	OA could not be assessed due to extensive anterior segment abnormalities
20	c.2430C>A p.(Phe810Leu), de novo	4	26	F	OA (9), DM (5), HL (0), cataract (2)	Also harbors c.683G>A, p.(Arg228His), a likely benign variant in trans
21	c.2541C>G p.(Cys847Trp)	3	20	F	OA (13)	
22	c.2590G>A p.(Glu864Lys)	5	15	F	OA (15), HL (6), precocious puberty, developmental delay	

**Table 2.** Summary of the disease-associated *WFS1* variants in this cohort. M, male; F, female; OA, optic atrophy; HL, hearing loss; DM, diabetes Mellitus.

analysis and the clinical presentation, we considered the likely pathogenic variant responsible for the phenotype and changed her diagnosis from AR-WS to (AD) WFLS.

### Ophthalmological examination

The median age at diagnosis of optic neuropathy was 13 (Mean 21.4; range 4–67). The mean binocular BCVA at the last follow-up was 0.42 LogMAR (20/52 Snellen). Visual acuity deteriorated slowly but remained in most patients below 0.58 LogMAR (above 20/76 Snellen, 75<sup>th</sup> percentile) (Fig. 1). A line chart of the visual acuity

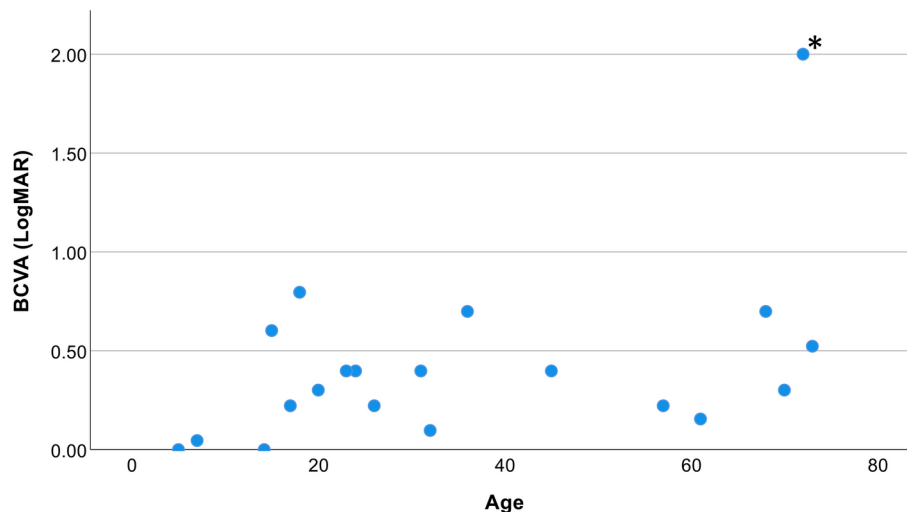


**Fig. 1.** Best-corrected binocular visual acuity (BCVA) of 20 patients per age at last follow-up. Mean BCVA was 0.42 LogMAR (20/52 Snellen), median 0.34 LogMAR (20/43 Snellen) and range 0–2. Seventy five percent of the patients had a BCVA lower than 0.58 LogMAR (20/76 Snellen). \*Patient 9 had, in addition to optic atrophy, corneal band keratopathy in the left eye and vitreomacular traction in both eyes but was not treated operatively because potential visual gain was expected to be insignificant.

versus age per patient is presented in supplementary Fig. 1. Nine patients (41%) had myopia with a mean spherical refraction of  $-5.4 \pm 4.4$  D.

Red-green color vision disturbances were observed in eight cases (36%), with an additional two cases (9%) presenting both red-green and blue-yellow color vision disturbances. Normal color vision was noted in four patients (18%), while reliable color vision testing was not feasible in two cases (9%). The color vision status remained unknown for six patients (27%). Notably, none of the patients exhibited isolated blue-yellow color vision disturbances.

Three patients (18%) developed juvenile/presenile cataract at the ages of 2, 3, and 32, respectively.

Funduscopy of patient 19 proved impossible due to extensive anterior chamber abnormalities. This newborn boy with variant p.Glu809Lys was born dysmature following an uncomplicated pregnancy and parturition. He had various dysmorphic features, such as congenital hand deformities with adduction contracture of thumbs and windblown fingers, persistent left superior vena cava, and congenital clubfoot. He also suffered from congenital HL and congenital DM. He had severe anterior segment abnormalities. The pupil was absent and there was no formed anterior chamber on slit lamp examination because of complete iridocorneal adhesion. On ultrasound imaging, the iris had a cystoid appearance and was confirmed to be completely adhered to the corneal endothelium (Supplementary Fig. 2).

OCT imaging of the macula and optic nerve head was available in 17 patients. Thirteen out of 17 patients (76.5%) showed a lamination of the outer plexiform layer which was characterized by two hyperreflective lines divided by one irregular hyporeflective line on macular OCT images (Fig. 2A). Intraretinal cystoid changes were observed in 11 patients (65%).

Twelve patients had pattern reversal VEP (prVEP) measurements according to ISCEV standards. prVEPs showed a delayed P100 peak time in 8 patients, 7 of which also had low amplitudes. Three patients had completely normal prVEPs; these patients had a BCVA of 0.0 LogMAR (20/20 Snellen) at the time of the VEP recording. A diagnosis of optic neuropathy in these patients was suspected on fundus examination and OCT findings, showing pale optic discs and thinning of the retinal nerve fiber layer, respectively.

Visual field assessments were available for 16 patients. Five patients showed central/paracentral scotomas, and 7 patients had peripheral constriction of the visual field or peripheral scotomas. Four patients had normal visual fields.

### Comparison of AD *WFS1*-OA versus DOA

We compared AD *WFS1*-OA patients with 22 age-matched DOA patients with genetically confirmed *OPA1* variants. In the DOA group, 9% had HL.

There was no significant difference in the BCVA of AD *WFS1*-OA ( $M=0.42$ ,  $SD=0.43$ ) and DOA ( $M=0.41$ ,  $SD=0.23$ ) patients at the last follow up ( $t(40)=0.41$ ,  $p=0.96$ ). Fisher's exact test showed that AD *WFS1*-OA patients were more likely to develop red-green color vision disturbance, while a blue-yellow color vision disturbance was more common in DOA patients ( $p=0.001$ ).

An analysis of variance using ANOVA to compare the retinal nerve fiber layer (RNFL) thickness between AD *WFS1*-OA patients, DOA patients and healthy controls revealed a thinner RNFL in all quadrants of the optic nerve in DOA and AD *WFS1*-OA patients compared to healthy controls ( $F(2,95)=69.8$ ,  $p=0.001$  for temporal RNFL;  $F(2,94)=94.4$ ,  $p=0.001$  for superior;  $F(2,95)=29.9$ ,  $p=0.001$  for nasal and  $F(2,95)=103.4$ ,  $p=0.001$  for inferior). A post hoc Tukey test showed that AD *WFS1*-OA patients had a thinner RNFL in all

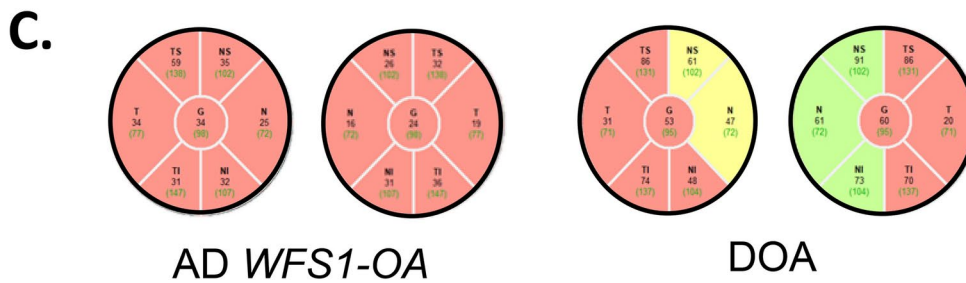
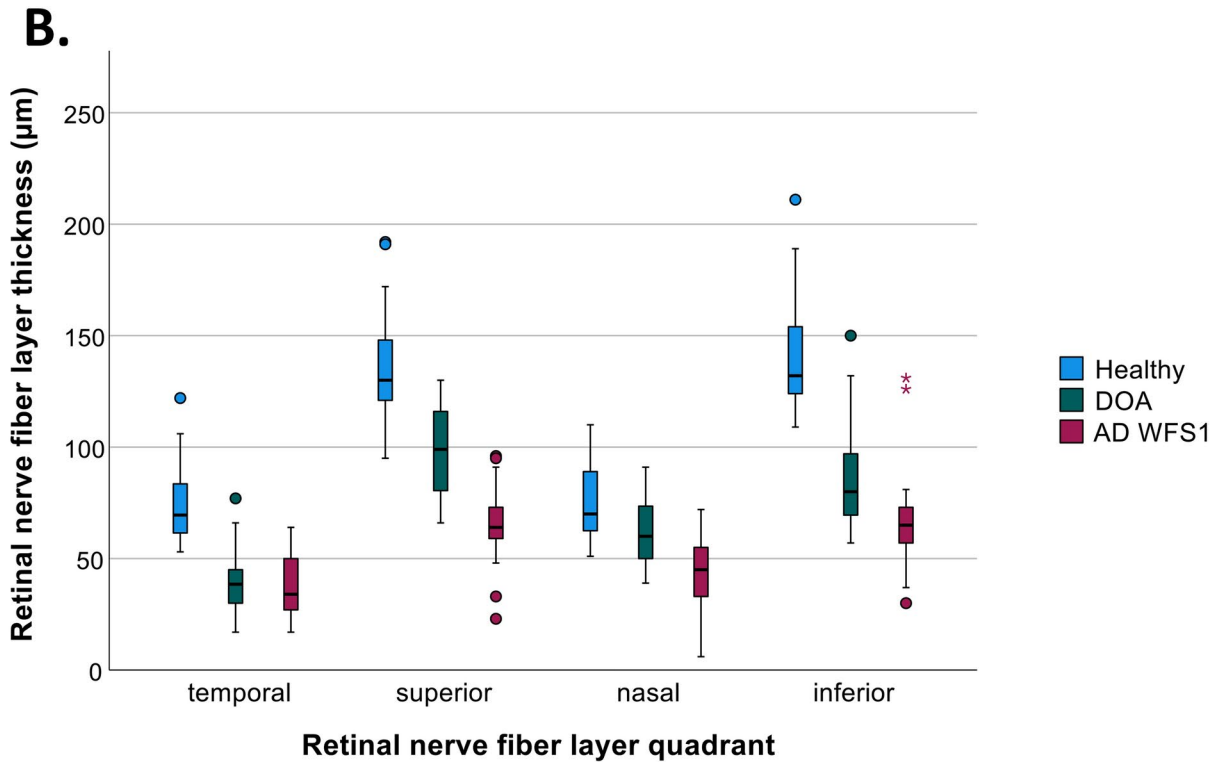
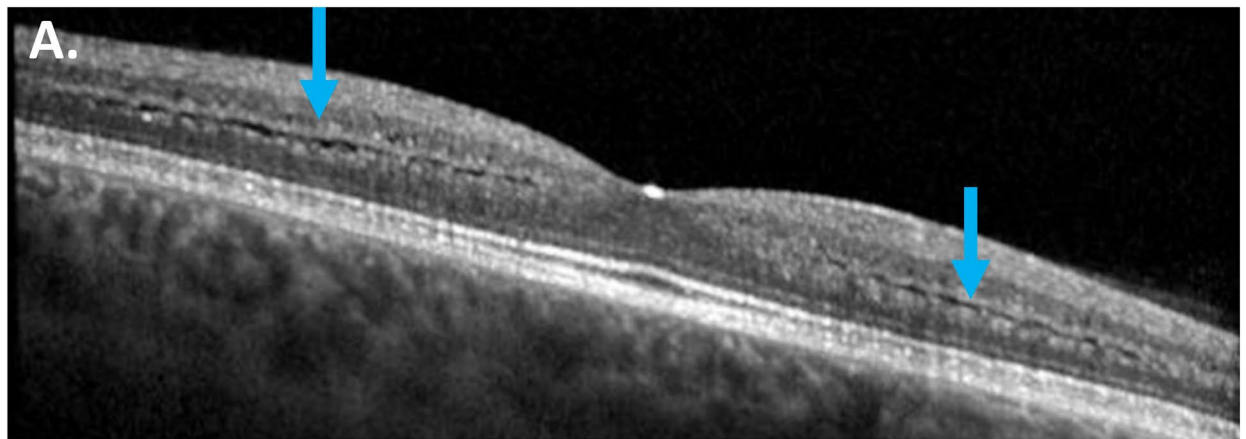


**Fig. 2.** OCT features of autosomal dominant *WFS1*-associated optic neuropathy (AD *WFS1*-OA) and dominant optic atrophy (DOA). **A.** Lamination of the outer plexiform layer (blue arrows) in an AD *WFS1*-OA case. **B.** Comparison of peripapillary retinal nerve fiber layer thickness in healthy controls, DOA and AD *WFS1*-OA patients. Compared to DOA patients, thinning of retinal fiber nerve layer (RNFL) was more severe in AD *WFS1*-OD patients in all quadrants, with the exception of the temporal quadrant. **C.** Two examples of typical peripapillary RNFL patterns in patients with AD *WFS1*-OA and DOA.

quadrants compared to DOA patients, except for the temporal quadrant ( $p=0.818$ ), in which the thinning was comparable (Fig. 2B,C). RNFL thinning was observed before the deterioration of visual acuity in four AD *WFS1*-OA patients. Details of the RNFL thickness measurements can be found in supplementary table 2.

Abnormal prVEPs in AD *WFS1*-OA patients consisted of delayed as well as small p100 responses while DOA patients showed mainly p100s with low amplitude but normal peak times. The observed differences of the prVEP were statistically not significant. A summary of these findings can be seen in Table 3.

## Discussion

In this study, we describe the clinical and the ophthalmological features of 21 patients with AD *WFS1*-OA (plus 1 patient with an unusual ocular phenotype) and compare these to *OPA1*-associated DOA. There were several notable ophthalmic phenotypic differences between AD *WFS1*-OA and DOA. AD *WFS1*-OA patients had more often red–green color vision disturbance, a pathognomonic OPL lamination on the macular OCT, and more widespread peripapillary RNFL thinning patterns compared to DOA patients. These differences can help to clinically distinguish AD *WFS1*-OA from DOA. Although patients with AD *WFS1*-OA frequently had accompanying non-ocular manifestations such as congenital or very early-onset HL (82%) and DM (32%), 4 patients had isolated OA, showing the importance of a clinical distinction from DOA.

Even when the exact mechanism is still unknown, the pathophysiology of AR and AD *WFS1*-OA appears to be a complex process that differs from other inherited ONs. Most inherited ONs are caused by genetic alterations in genes with a direct mitochondrial function. In contrast, wolframin, the protein encoded by *WFS1*, is an endoplasmic reticulum protein with indirect involvement in respiratory functions. A growing body of evidence suggests that in the wolframinopathies the axonal degeneration precedes retinal ganglion cell (RGC) loss, in some cases up to a decade<sup>10–13</sup>. This is different from DOA, for example, where RGC loss is already present in the early years of life and more prominent than the thinning of RNFL<sup>14</sup>. In a recent study by Rossi and coworkers, the optic nerves of homozygous *WFS1* mutant mice showed myelin disorganization, neuroinflammation, and abnormalities in lactate shuttling between oligodendrocytes and RGC axons, a metabolic exchange mechanism that is important for the energy supply of the RGC axons in times of high energy needs. This pathological process with the involvement of myelin may explain the different clinical features of AD *WFS1*-OA, such as more prominently delayed p100 on prVEPs, compared to DOA. A widespread neuroinflammatory process affecting the whole optic nerve rather than local RGC loss might also explain the higher frequency of red–green color vision disturbance in AD *WFS1*-OA. Acquired red–green color vision disturbance is also commonly seen in other demyelinating diseases, such as optic neuritis in multiple sclerosis<sup>15–17</sup>.

In DOA patients, the peripapillary RNFL thickness reduction is in general more prominent at the temporal side of the optic nerve<sup>10,18–22</sup>. In our study cohort, AD *WFS1*-OA patients had extensive reduction of RNFL thickness without a recognizable topographic preference. In a recent study, Barboni and co-workers compared the pattern of RGC loss in AR-WS patients with DOA patients<sup>10</sup>. In this study, DOA patients had thicker RNFL in all sectors except for the temporal sector compared to AR-WS patients, similar to our findings. These findings underline the different patterns of RGCs degeneration in the presence of *WFS1* variants, in AR as well as AD disease, compared to other common inherited ONs.

Two patients (Patient 2 and 20) in this cohort had two variants in *WFS1*, and they were referred to an ophthalmologist with the diagnosis of AR-WS. However, detailed clinical and ophthalmologic phenotyping was more in line with AD *WFS1*-associated disease in both patients (congenital HL, OPL lamination, cataract at early age, and no systemic involvement except DM in one)<sup>4</sup>. In one patient, the genetic testing was performed in 2001, and the reassessment of the variants designated one variant as likely benign and one as likely pathogenic. In the other patient, segregation analysis revealed two variants on the same allele with one being a de novo

Ophthalmological feature	AD <i>WFS1</i> -OA	DOA	p-value
BCVA at last follow up (mean ± SD)	0.42 ± 0.43	0.41 ± 0.23	0.96
Color vision			
Red–green	<b>8 (36%)</b>	1 (5%)	<b>0.001</b>
Blue–yellow	0 (0%)	<b>8 (36%)</b>	
Mixed	2 (10%)	4 (18%)	
Normal	4 (18%)	1 (5%)	
OCT			
Macula	OPL lamination	Normal OPL	NA
Optic nerve head	Global thinning of RNFL	More prominent thinning of temporal RNFL	
PrVEP (BE, 15°)			
Amplitude p100 (n/total)	Low (7/12)	<b>Low (11/13)</b>	0.25
	Normal (5/12)	Normal (2/13)	
Latency p100 (n/total)	<b>Prolonged (8/12)</b>	Prolonged (3/13)	0.06
	Normal (4/12)	Normal (10/13)	

**Table 3.** Summary of the comparison in ophthalmologic findings in autosomal dominant *WFS1*-associated optic neuropathy versus *OPA1*-associated dominant optic atrophy. PrVEP, pattern reversal visually evoked potentials; BE, recording of both eyes with 15° block size.

mutation, so that AD disease was confirmed in both cases. These two examples underline the importance of detailed phenotyping and thorough genetic assessment. Although the clinical pictures of AR and AD *WFS1*-associated disease have a certain degree of overlap, AD *WFS1*-associated disease has, in general, less severe systemic involvement and presents predominantly with sensory symptoms, isolated or combined<sup>4</sup>. Thus, it is important to differentiate these wolframopathies to be able to provide a more accurate prognosis and genetic counselling.

Four patients (Patient 3, 4, 16 and 21) in this study presented with isolated OA, without any other phenotypic feature of *WFS1*-associated disease. Interestingly, these patients showed no OPL lamination on the macular OCT. Three of them harbored pathogenic *WFS1* variants with an unequivocal genetic diagnosis, and only in one patient the detected *WFS1* variant was classified as variant of unknown significance. Although rare, isolated optic neuropathy in *WFS1* variants was previously reported by Grenier et al. in recessive state<sup>23</sup>. The c.1672C>T (p.Arg558Cys) variant in patient 3, who is Belgian of Ashkenazi Jewish ethnicity, has a high allele frequency in Ashkenazi Jewish population (%1,5), obscuring the variant classification as disease associated in AD state. However, it was previously described by Yarkoni et al. in association with a milder, later onset Wolfram syndrome phenotype in 8 patients in homozygous state<sup>24</sup>. Pathogenic variants in the 2 other patients were also previously described in AR disease. Patient 4 had a pathogenic variant and was related to a patient with WS with compound heterozygous variants. Patient 21 was heterozygous carrier of the class 3 variant c.2541C>G p.(Cys847Trp) and her mother had also isolated optic atrophy, prompting an inherited cause for the disease. The mother was compound heterozygous with one more class 3 *WFS1* variant and therefore was excluded from this study. We hypothesize that some *WFS1* variants that cause complete AR-WS in biallelic state, may pose as risk factor to develop optic atrophy in the heterozygous state as a part of multifactorial disease etiology. Increased penetrance in some AR variants can also be an explanation. We do not have evidence in the current study to support this hypothesis but, if true, it would also explain the absence of the OPL lamination on the OCTs of these patients as the structural changes in retina are different in AR and AD disease. Whether the mode of inheritance can be named as AD in this group is still debatable and more research with functional studies are needed to confirm the pathogenicity of these variants in heterozygous state.

The findings of the current study confirm the findings of our recently published systematic review on AD WFLS where we defined the main phenotypic presentation of Wolfram-like syndrome as optic atrophy and congenital HL<sup>4</sup>. One patient with unusual phenotypic features (microphthalmia, bilateral microcornea, and iris coloboma; bilateral clubfeet, left thumb contracture) was excluded from that systematic review because such a phenotype had not been described before, and because of uncertain causality of *WFS1* in the development of all the clinical features.<sup>25</sup> However, in the current study we encountered a patient with a very similar phenotype in the presence of the same variant (c.2425G>A p.(Glu809Lys)). This supports the association of the p.(Glu809Lys) variant with a severe and atypical phenotype, characterized by anterior segment dysgenesis and extremity anomalies, next to well-known *WFS1* related manifestations.

This study has a few limitations due to its retrospective design. Yet, we believe that it contributes substantially to the phenotyping of a rare disease. Prospective natural history studies and laboratory studies in heterozygous mutant disease models are needed to gain an in-depth understanding the pathophysiological processes behind this intriguing group of diseases. Longitudinal analysis of the OPL and RGC using macular EDTRS grid could be an interesting next step to explore the development of the OPL lamination.

In conclusion, *WFS1* variants can cause a spectrum of phenotypes, which we have collectively named the 'wolframopathies'<sup>4</sup>. Biallelic *WFS1* variants are associated with AR-WS while single heterozygous variants are associated with ophthalmologic presentations in the form of AD Wolfram-like syndrome, AD Wolfram-like syndrome with hand, foot, and ocular dysgenesis and possibly isolated OA without OPL lamination. Thorough ophthalmic phenotyping can aid in distinguishing AD *WFS1*-OA from DOA+, as two diseases present with a similar phenotype but slightly different structural and functional changes.

## Materials and methods

### Patient population and genetic analysis

Patients were included in the study if they had at least one ophthalmologic phenotypic feature previously described for *WFS1*-associated disease, and genetic confirmation of a heterozygous variant in *WFS1*. Exclusion criteria were other possible causes explaining optic atrophy.

The study was approved by the ethical review board of the Academic Medical Center, Amsterdam University Medical Centers, and executed according to the tenets of the Declaration of Helsinki. Patients were recruited from the Amsterdam University Medical Centers, Bartiméus Diagnostic Center Zeist, Rotterdam Eye Hospital, Erasmus Medical Center, University Medical Center Groningen, University Medical Center Utrecht, and Leiden University Medical Center in the Netherlands, and from Ghent University Hospital in Belgium. Informed consent was obtained from the patients according to the local regulations in the country where the recruitment took place. In minor participants, informed consent was taken from the parents/guardians.

Genetic analyses were performed in the Amsterdam University Medical Centers, Amsterdam (the Netherlands), Radboud University Medical Center, Nijmegen (the Netherlands), and Ghent University Hospital, Ghent (Belgium). Patients were diagnosed with either next generation sequencing panels (NGS) analyzing genes known to be involved in inherited ONs, or with larger NGS panels for blindness covering 256 genes associated with genetic eye diseases. NGS panel for inherited ON included ACO2, AUH, C12Orf65, CISD2, MFN2, MTPAP, NBAS, NDUFS1, NR2F1, OPA1, OPA3, RTN4IP1, SLC25A46, SPG7, TIMM8A, TMEM126A, WFS1, SLC24A1 and the 3 mitochondrial mutations m.3460G>A (MT-ND1), m.11778G>A (MT-ND4) and m.14484T>C (MT-ND6). Variant assessment was performed based on institutional guidelines in line with the American College of Medical Genetics classification.

## Clinical assessment and data collection

Clinical data of 22 patients were obtained retrospectively from multiple study sites by reviewing the medical records of the patients. Collected data included: demographics (age, sex, country of origin), family history, extraocular manifestations, age at onset, best-corrected visual acuity (BCVA), refractive error, visual field testing, color vision testing, spectral domain optical coherence tomography (OCT) imaging of the macula and optic nerve head, color fundus photography, and visually evoked potentials (VEP). OCT data of 16 age-matched, anonymous, healthy subjects and clinical data of 22 age-matched, anonymous DOA patients with confirmed (likely) disease-causing/pathogenic *OPA1* variants were collected from the patient registers from Bartiméus Diagnostic Center and Amsterdam University Medical Centra for comparison.

Visual acuity was measured with Snellen charts and converted to logMAR units for data analysis. Visual fields were assessed using manual Goldmann kinetic perimetry, automated static Humphrey Visual Field Analyzer (Carl-Zeiss Meditec, Dublin, CA, USA), or Octopus visual field perimetry (Octopus perimeter, Haag-Streit International, Switzerland). Either Canon Xephilio OCT-A1 (Canon Inc., Kanagawa, Japan) or Spectralis OCT (Heidelberg Engineering GmbH, Heidelberg, Germany) were used to perform OCT imaging. Color vision was assessed with HRR Pseudoisochromatic Plates. Pattern reversal VEPs were recorded according to the International Society for Clinical Electrophysiology of Vision (ISCEV) standards with an Espion E3 system (Diagnosys LLC, Cambridge, UK) or a RETI-port/scan 21 system (Roland Consult, Brandenburg an der Havel, Germany)<sup>26</sup>.

## Statistical analysis

Statistical analyses were performed using SPSS statistical software (version 28.0 for Windows, SPSS Inc., Chicago, IL, USA). Missing data were handled based on pairwise deletion. Categorical data were assessed either with Chi-Square test, or with Fisher's exact test depending on sample size and were presented as proportions. Continuous data were reported as mean or median with ranges. For pairwise comparison of multiple groups, one-way ANOVA test was performed with Tukey's HSD as post hoc analysis.

## Data availability

The datasets generated during and/or analyzed during the current study are available from the corresponding author on reasonable request.

Received: 3 July 2024; Accepted: 25 September 2024

Published online: 03 October 2024

## References

- Inoue, H. *et al.* A gene encoding a transmembrane protein is mutated in patients with diabetes mellitus and optic atrophy (Wolfram syndrome). *Nat. Genet.* **20**, 143–148. <https://doi.org/10.1038/2441> (1998).
- Strom, T. M. *et al.* Diabetes insipidus, diabetes mellitus, optic atrophy and deafness (DIDMOAD) caused by mutations in a novel gene (wolframin) coding for a predicted transmembrane protein. *Hum. Mol. Genet.* **7**, 2021–2028. <https://doi.org/10.1093/hmg/7.13.2021> (1998).
- Eiberg, H. *et al.* Autosomal dominant optic atrophy associated with hearing impairment and impaired glucose regulation caused by a missense mutation in the WFS1 gene. *J. Med. Genet.* **43**, 435–440. <https://doi.org/10.1136/jmg.2005.034892> (2006).
- deMuijnck, C., Brink, J. B., Bergen, A. A., Boon, C. J. F. & vanGendren, M. M. Delineating Wolfram-like syndrome: A systematic review and discussion of the WFS1-associated disease spectrum. *Surv. Ophthalmol.* **68**, 641–654. <https://doi.org/10.1016/j.survophthal.2023.01.012> (2023).
- Grenier, J. *et al.* WFS1 in optic neuropathies: Mutation findings in nonsyndromic optic atrophy and assessment of clinical severity. *Ophthalmology* **123**, 1989–1998. <https://doi.org/10.1016/j.ophtha.2016.05.036> (2016).
- Hoekel, J. *et al.* Visual pathway function and structure in Wolfram syndrome: patient age, variation and progression. *BMJ Open Ophthalmol.* **3**, e000081. <https://doi.org/10.1136/bmjophth-2017-000081> (2018).
- Majander, A. *et al.* Lamination of the outer plexiform layer in optic atrophy caused by dominant WFS1 mutations. *Ophthalmology* **123**, 1624–1626. <https://doi.org/10.1016/j.ophtha.2016.01.007> (2016).
- Majander, A. *et al.* WFS1-associated optic neuropathy: genotype-phenotype correlations and disease progression. *Am. J. Ophthalmol.* **241**, 9–27. <https://doi.org/10.1016/j.ajo.2022.04.003> (2022).
- Rocatcher, A. *et al.* The top 10 most frequently involved genes in hereditary optic neuropathies in 2186 probands. *Brain* **146**, 455–460. <https://doi.org/10.1093/brain/awac395> (2023).
- Barboni, P. *et al.* The pattern of retinal ganglion cell loss in wolfram syndrome is distinct from mitochondrial optic neuropathies. *Am. J. Ophthalmol.* **241**, 206–216. <https://doi.org/10.1016/j.ajo.2022.03.019> (2022).
- Plaas, M. *et al.* Wfs1-deficient rats develop primary symptoms of Wolfram syndrome: Insulin-dependent diabetes, optic nerve atrophy and medullary degeneration. *Sci. Rep.* **7**, 10220. <https://doi.org/10.1038/s41598-017-09392-x> (2017).
- Rossi, G. *et al.* MCT1-dependent energetic failure and neuroinflammation underlie optic nerve degeneration in Wolfram syndrome mice. *Elife* <https://doi.org/10.7554/eLife.81779> (2023).
- Lugar, H. M. *et al.* Neuroimaging evidence of deficient axon myelination in Wolfram syndrome. *Sci. Rep.* **6**, 21167. <https://doi.org/10.1038/srep21167> (2016).
- Barboni, P. *et al.* Retinal nerve fiber layer thickness in dominant optic atrophy: Measurements by optical coherence tomography and correlation with age. *Ophthalmology* **118**, 2076–2080. <https://doi.org/10.1016/j.ophtha.2011.02.027> (2011).
- Piro, A. *et al.* Impairment of acquired color vision in multiple sclerosis: an early diagnostic sign linked to the greatness of disease. *Int. Ophthalmol.* **39**, 671–676. <https://doi.org/10.1007/s10792-018-0838-x> (2019).
- Katz, B. The dyschromatopsia of optic neuritis: A descriptive analysis of data from the optic neuritis treatment trial. *Trans. Am. Ophthalmol. Soc.* **93**, 685–708 (1995).
- Schneck, M. E. & Haegerstrom-Portnoy, G. Color vision defect type and spatial vision in the optic neuritis treatment trial. *Invest. Ophthalmol. Vis. Sci.* **38**, 2278–2289 (1997).
- Rönnbäck, C., Milea, D. & Larsen, M. Imaging of the macula indicates early completion of structural deficit in autosomal-dominant optic atrophy. *Ophthalmology* **120**, 2672–2677. <https://doi.org/10.1016/j.ophtha.2013.08.008> (2013).
- Asanad, S. *et al.* Optical coherence tomography of the retinal ganglion cell complex in Leber's hereditary optic neuropathy and dominant optic atrophy. *Curr. Eye Res.* **44**, 638–644. <https://doi.org/10.1080/02713683.2019.1567792> (2019).



20. Yu-Wai-Man, P., Bailie, M., Atawan, A., Chinnery, P. F. & Griffiths, P. G. Pattern of retinal ganglion cell loss in dominant optic atrophy due to OPA1 mutations. *Eye (Lond)***25**, 596–602. <https://doi.org/10.1038/eye.2011.2> (2011).
21. Barboni, P. *et al.* Retinal nerve fiber layer thickness in dominant optic atrophy measurements by optical coherence tomography and correlation with age. *Ophthalmology***118**, 2076–2080. <https://doi.org/10.1016/j.ophtha.2011.02.027> (2011).
22. Corajevic, N., Larsen, M. & Rönnebäck, C. Thickness mapping of individual retinal layers and sectors by spectralis SD-OCT in autosomal dominant optic atrophy. *Acta Ophthalmol.***96**, 251–256. <https://doi.org/10.1111/aos.13588> (2018).
23. Grenier, J. *et al.* WFS1 in optic neuropathies: mutation findings in nonsyndromic optic atrophy and assessment of clinical severity. *Ophthalmology***123**, 1989–1998 (2016).
24. Wilf-Yarkoni, A. *et al.* Mild phenotype of wolfram syndrome associated with a common pathogenic variant is predicted by a structural model of wolframin. *Neurol. Genet.***7**, e578. <https://doi.org/10.1212/nxg.0000000000000578> (2021).
25. De Franco, E. *et al.* Dominant ER stress-inducing WFS1 mutations underlie a genetic syndrome of neonatal/infancy-onset diabetes, congenital sensorineural deafness, and congenital cataracts. *Diabetes***66**, 2044–2053. <https://doi.org/10.2337/db16-1296> (2017).
26. Odom, J. V. *et al.* ISCEV standard for clinical visual evoked potentials: (2016 update). *Doc. Ophthalmol.***133**, 1–9. <https://doi.org/10.1007/s10633-016-9553-y> (2016).

### Author contributions

C.d.M.: Investigation, formal analysis, writing original draft, visualization; L.H.W. and E.d.B.: analysis of the genetic data; J.A.M.v.E., T.L., P.A.T.H., M.F.v.D., A.J.A.K., V.J.M.V., M.E.H.S., R.A.W., I.C.N., S.W., J.d.Z.; F.v.d.B. and B.P.L.: data acquisition, writing- reviewing; C.J.F.B. and M.M.v.G.: supervision, conceptualization, methodology, writing- reviewing and editing. All authors reviewed the manuscript.

### Competing interests

The authors declare no competing interests.

### Additional information

**Supplementary Information** The online version contains supplementary material available at <https://doi.org/10.1038/s41598-024-74364-x>.

**Correspondence** and requests for materials should be addressed to M.M.G.

**Reprints and permissions information** is available at [www.nature.com/reprints](http://www.nature.com/reprints).

**Publisher's note** Springer Nature remains neutral with regard to jurisdictional claims in published maps and institutional affiliations.

**Open Access** This article is licensed under a Creative Commons Attribution-NonCommercial-NoDerivatives 4.0 International License, which permits any non-commercial use, sharing, distribution and reproduction in any medium or format, as long as you give appropriate credit to the original author(s) and the source, provide a link to the Creative Commons licence, and indicate if you modified the licensed material. You do not have permission under this licence to share adapted material derived from this article or parts of it. The images or other third party material in this article are included in the article's Creative Commons licence, unless indicated otherwise in a credit line to the material. If material is not included in the article's Creative Commons licence and your intended use is not permitted by statutory regulation or exceeds the permitted use, you will need to obtain permission directly from the copyright holder. To view a copy of this licence, visit <http://creativecommons.org/licenses/by-nc-nd/4.0/>.

© The Author(s) 2024